

## FLEXURAL TENSILE BEHAVIOUR OF ENHANCED PERFORMANCE CONCRETE

A. CAMÕES\*, J. BARROS\*, B. AGUIAR\*

\*Department of Civil Engineering  
Universidade do Minho  
Azurém, 4800-058 Guimarães

**Abstract.** High-performance concrete is generally produced using carefully selected high quality materials. These materials increase significantly the initial costs, hence, limiting its use. In this research work the performance of concrete was enhanced through incorporating low cost untreated materials like fly ash and crushed aggregates. Thus, it can be produced enhanced or even high performance low cost concrete and, also, decrease significantly the use of cement and non-renewable natural resources (river/sea sand), contributing to the necessary sustainability of construction. From experimental program, the effect of replacing cement by fly ash (up to 60%) in the flexural tensile behaviour was evaluated, using control compositions without the addition of fly ash as a base of comparison. The results obtained demonstrate that it is possible to produce enhanced performance concrete with the selected materials replacing up to 40% of the cement by fly ash. In specimens of such mixtures, cured at least 56 days, the values of the compressive strength and the flexural tensile parameters were similar to the ones of the control mixtures.

### 1. INTRODUCTION

The performance of a cement-based material is usually assessed from its compressive strength.

Nevertheless, the accuracy of a numerical simulation of the behaviour of a concrete structure depends on the quality of the constitutive laws used to model the concrete post-cracking behaviour [1], [2]. This law is defined from the concrete fracture parameters.

Uniaxial tensile test is the most appropriate to evaluate the values of these parameters. However, to assure stable tests in the strain softening phase, high stiff reaction frames and equipment including sophisticated control algorithms are needed, resulting a test set-up not available in the majority of the laboratories [3].

Flexural tensile test do not require so level of sophistication, and can be used to evaluate the material fracture energy, a key property amongst the fracture parameters. To carry out stable flexural tests, servo-controlled equipment was developed in the last years in the Laboratory of the Department of Civil Engineering of University of Minho. This equipment was used to determine the full flexural behaviour of enhanced performance concretes. The influence of the amount of binder (500 and 600 kg/m<sup>3</sup>), the percentage of cement replaced by fly ash (0, 20%, 40% and

60%), as well as the concrete age (7, 28, 56 and near 160 days) on the flexural post-cracking behaviour were assessed carrying out three-point bending tests with notched beams. The results obtained are presented and analysed.

### 2. MATERIALS, MIXTURE PROPORTIONS, MANUFACTURE AND CURING

All the aggregates used in this research work were obtained from crushed granite of the same quarry. Two sands of maximum aggregate sizes ( $D_{max}$ ) of 2.38 mm (Sand 1) and 4.76 mm (Sand 2), and a coarse aggregate of  $D_{max}$  of 9.53 mm were used as received, without any treatment.

Ordinary Portland cement (C) type CEM I 42,5R was used.

The fly ash (FA) was supplied by the Portuguese Thermoelectric Power Plant of Pego. The quantities of loss on ignition (LOI) varied between 6% and 9%, resulting in an average value over 7%. The LOI value is higher than the maximum allowed by the European Standard EN450 [4] and the American Standard ASTM C618 [5], which limit LOI to 5% and 6% respectively. This would mean that the FA used in this work

could be considered as a poor quality FA, with high carbon content.

The superplasticizer (SP) had a chemical composition based on naphthalene sulphonate formaldehyde condensates. In previous works [6-8], the optimum superplasticizer solid content was estimated to be between 0.5% and 1.0% of the mass of binder. Due to economic reasons, the value of 0.5% was adopted in this research work.

More details of the main characteristics of the materials are elsewhere [6-8].

Eight different mixes corresponding to two binder contents and four levels of cement replacement were used. Binder contents (B) of 500 kg/m<sup>3</sup> and 600 kg/m<sup>3</sup> were adopted and the

corresponding water/binder ratio, W/B, was 0.3 and 0.25. The mix composition was determined using the Faury method, resulting the compositions presented in table 1, where the workability obtained using the Slump and the Flow Table tests were also indicated.

The mnemonic abbreviation used has the following meaning: the first number refers to the amount of binder and the number that follows FA represents the percentage of cement replaced by FA.

Cylindrical specimens of 150 mm diameter and 300 mm height were moulded in order to evaluate the compressive strength of the concrete compositions. The flexural behaviour was assessed using 850x100x100 mm<sup>3</sup> beam specimens.

**Table 1** – Concrete mix proportions and workability

Concrete	W/B	C (kg/m <sup>3</sup> )	FA (kg/m <sup>3</sup> )	Sand 1 (kg/m <sup>3</sup> )	Sand 2 (kg/m <sup>3</sup> )	Coarse Aggregate (kg/m <sup>3</sup> )	Slump (mm)	Flow Table (mm)
500FA0	0.30	500	0	503	308	865.61	25	315
500FA20	0.30	400	100	462	334	869.82	105	395
500FA40	0.30	300	200	407	349	847.11	205	474
500FA60	0.30	200	300	364	374	848.70	230	550
600FA0	0.25	600	0	377	368	850.73	35	350
600FA20	0.25	480	120	326	400	856.01	125	365
600FA40	0.25	360	240	271	408	832.76	200	510
600FA60	0.25	240	360	223	421	824.23	230	530

The specimens were placed into a curing room, at a temperature of 21°C and a constant relative humidity of 80%. The specimens were demoulded 24 hours after have been cast, and were immersed in water at 21° until their preparation for testing.

In the pre-test preparation phase of beam specimens, a notch of 5 mm width and 25 mm depth was sawn in a beam face parallel to the casting direction.

### 3. TEST PROCEDURE

The flexural behaviour of the produced concretes was evaluated carrying out three-point bending tests according to RILEM recommendations [2].

Loading, support conditions and the arrangement of the displacement transducers (LVDTs) are show in figures 1 and 2. The tests

were controlled by LVDT1 of 5 mm of linear measuring length and 0.05% of accuracy. A Japanese-Yoke-system was used to avoid that LVDT1 has registered extraneous displacements [10] (see figure 1b). LVDT2 and LVDT3 were placed according to figure 1c for the estimation of the deformations at the fracture zone. LVDT2 had 5 mm of linear measuring length and 0.09% of precision, while LVDT3 had 6.3 mm of linear measuring length and 0.05% of precision.

A load cell of 10000 N of bearing capacity and 0.05% of precision was used to measure the force.

All the tests were performed with a mid-span deflection increase at a constant rate of 0.36 mm/min.

The tests were carried out using closed loop equipment developed in the University of Minho [9].

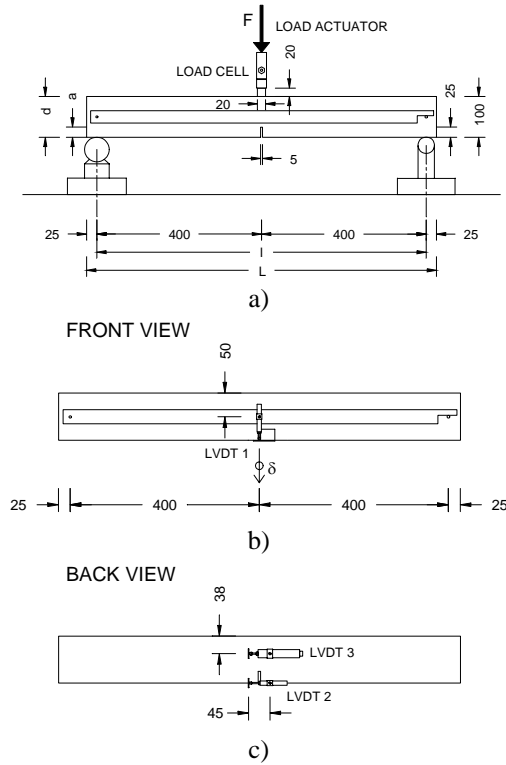


Fig. 1 – Three-point bending test set-up scheme

The stiffness of the test reaction frame and the gain of the test controller device should be defined to avoid unstable zones in the test softening phase. These aspects are particularly important when testing fragile specimen's materials like enhanced performance concretes. Definitions of these characteristics were investigated in previous works [10] and stable tests were performed in all specimens.

The compressive strength of the produced concretes was evaluated from uniaxial compression tests carried out in a closed-loop servo controlled compression-testing machine. An LVDT of 5 mm linear measuring length and 0.09% of accuracy was used to control the test, at a displacement rate of 0.12 mm/min.

The fracture energy,  $G_F$ , was estimated from the equation proposed by RILEM [2]:

$$G_F = \frac{W_0 + (m_1(1 - \alpha^2) + 2m_2)g \delta_u}{b(d - a)} \quad (1)$$

where  $W_0$  is the work produced by the force  $F$  during the deformation of the specimen ( $\delta$ ), i.e. the area under the force-deflection curve,  $F-\delta$ . In (1),  $m_1$  is the mass of the specimen between the supports;  $m_2$  is the mass of a device, which weight is acting on the specimen and was not registered by the load cell;  $\alpha = L/l - 1$  is a parameter that corrects the work done by the

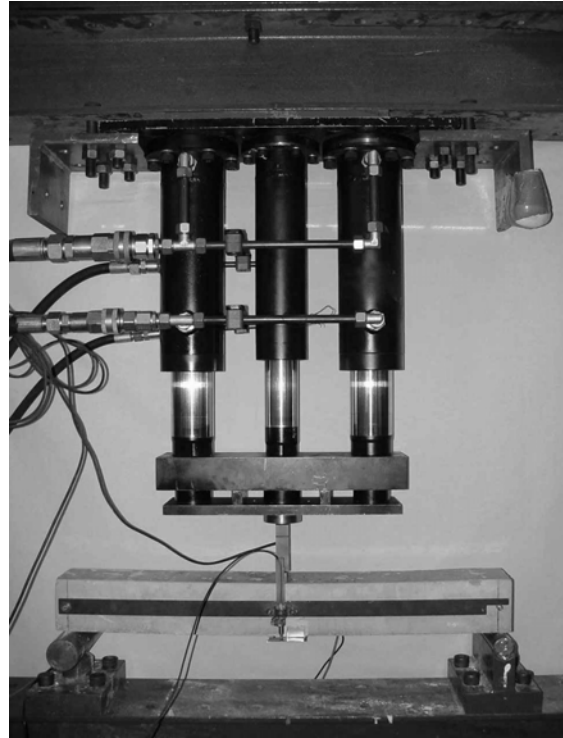


Fig. 2 – Three-point bending test photo

mass of the specimen itself;  $g$  is the gravity acceleration;  $\delta_u$  is the final deflection of the beam, i.e. the displacement recorded at the end of the test, where  $F = 0$ ; and  $b(d - a)$  is the cross-sectional area of beam above the notch.

Flexural strength can be calculated using the following expression [11]:

$$f_{c,fl} = 1.5 \frac{[F_{max} + 0.5m_1 g(1 - \alpha^2) + m_2 g]l}{b(d - a)^2} \quad (2)$$

In the present work, the flexural modulus of elasticity of the concrete specimens was calculated according to Petersson [12]:

$$E_{c,fl} = \left[ 1 + 3.15 \left( \frac{d}{l} \right)^2 + 8 \frac{d}{l} g \left( \frac{a}{d} \right) \right] \frac{1}{4b} \left( \frac{l}{d} \right)^3 \frac{dF}{d\delta} \quad (3)$$

where  $g(a/d)$  is a function that, for  $0.45 < a/d < 0.55$ , can be calculated by equation (4):

$$g \left( \frac{a}{d} \right) = \frac{0.15}{(1 - a/d)^3} \quad (4)$$

For  $a/d$  values not located in the defined interval, Hillerborg [13] suggested the values presented in table 2.

**Table 2** –  $g(a/d)$  values for  $0 < a/d < 0.5$ 

$a/d$	0.1	0.2	0.3	0.4	0.5
$g(a/d)$	0.035	0.14	0.32	0.63	1.20

In equation (3)  $dF/d\delta$  represent the slope of the linear branch of the flexure Force-deflection relationship.

**Table 3** – Experimental results

Concrete	Age	$f_{cm}$ (MPa)	$f_{cm,fl}$ (MPa)	$G_{Fm}$ (N/m)	$E_{cm,fl}$ (GPa)
500FA0	7	42.63	5.71	159.10	29.22
	28	45.41	6.08	183.69	29.57
	56	46.12	6.00	193.18	30.49
	165	57.59	6.28	203.92	31.81
500FA20	7	33.36	4.64	155.52	26.50
	28	40.83	5.65	165.49	26.65
	56	46.22	5.24	185.39	31.45
	165	58.96	5.29	198.42	30.01
500FA40	7	30.15	*	*	*
	28	35.54	*	*	*
	56	48.30	5.12	180.35	29.43
	165	61.32	5.70	191.64	32.27
500FA60	7	17.83	2.58	80.13	18.97
	28	28.13	3.28	126.42	23.45
	56	34.24	3.81	135.93	24.09
	165	49.20	4.34	174.62	25.71
600FA0	7	46.23	5.44	143.97	28.49
	28	53.16	5.69	191.26	29.21
	56	58.24	6.01	196.20	30.33
	157	66.99	5.95	198.32	31.48
600FA20	7	39.31	4.64	126.92	28.26
	28	50.76	5.01	183.11	29.25
	56	59.70	6.03	182.87	30.35
	157	69.46	6.13	186.53	31.29
600CV40	7	31.90	3.77	121.37	22.05
	28	45.09	4.68	161.75	26.77
	56	52.59	5.81	160.05	28.97
	157	74.53	5.66	180.53	29.92
600FA60	7	23.01	2.61	75.59	17.76
	28	36.26	4.31	125.01	23.22
	56	50.41	5.01	126.49	25.38
	157	60.05	5.22	155.46	25.52

\* Results not considered due to anomalies detected

#### 4. EXPERIMENTAL RESULTS AND ANALYSIS

Table 3 includes the main results obtained in the experimental program. Each value is the average of the results recorded in three specimens. In this table  $f_{cm}$  is the average compressive strength,  $f_{cm,fl}$  is the average flexure tensile strength,  $G_{Fm}$  is the average fracture energy and  $E_{cm,fl}$  is the average modulus of elasticity in flexure.

##### 4.1. Flexural tensile strength

Figure 3 shows the variation of flexural tensile strength,  $f_{cm,fl}$ , with the specimen's age and FA content. The results obtained indicate that:

a) For the designed compositions  $f_{cm,fl}$  remained practically constant for ages greater than 56 days. For compositions without FA,  $f_{cm,fl}$  remained constant after 28 days of curing. For compositions with  $B = 500 \text{ kg/m}^3$ , apart series 500FA60, marginal increments on the  $f_{cm,fl}$  were observed after 28 days. Similar trend was verified for  $B = 600 \text{ kg/m}^3$ , but only after 56 days of curing.

b) In the compositions with 60% of FA, values of  $f_{cm,fl}$  significantly smaller than the values recorded in the other mixtures were obtained. However, increasing the binder content from  $500 \text{ kg/m}^3$  to  $600 \text{ kg/m}^3$ ,  $f_{cm,fl}$  of compositions with 60% of FA became closer to the  $f_{cm,fl}$  values of the remaining compositions.

c) Increasing the binder content from 500 kg/m<sup>3</sup> to 600 kg/m<sup>3</sup> had a marginal effect on  $f_{cm,fl}$ . Only in compositions with 60% of

FA, the use of higher binder contents seems to be advantageous.

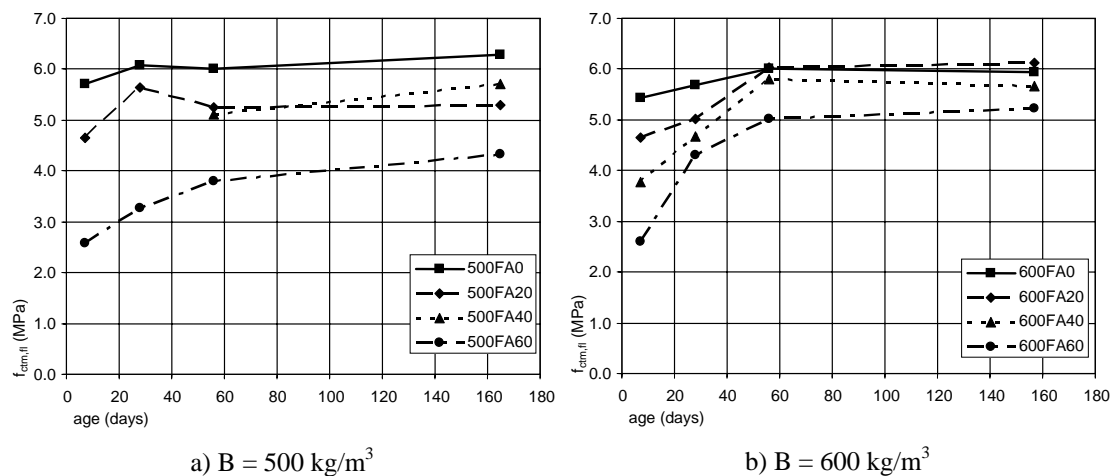


**Fig. 3** – Influences of the age and percentage of cement replaced by fly ash on the flexural-tensile strength

Figure 4 shows the compressive strength,  $f_{cm}$ , versus  $f_{cm,fl}$ .

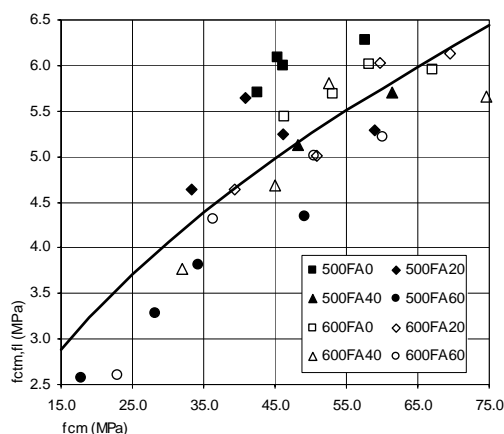


**Fig. 4** – Relation between compressive strength and flexural-tensile strength

The equation that best fits ( $R^2 = 0.70$ ) the overall results of the tested compositions is the following:

$$f_{cm,fl} = 0.7429\sqrt{f_{cm}} \quad (5)$$

For concretes of lower strength class, this expression predicts  $f_{cm,fl}$  values higher than the values recorded experimentally.

#### 4.2. Fracture energy

The influences of the age, binder content and FA on the  $G_{Fm}$  are represented in figure 5.

From this figure the following remarks can be pointed out:

a) The fracture energy increases with the age. For mixtures with FA lower than 60% and for ages longer than 56 days, however, the increase of  $G_{Fm}$  becomes negligible.

b) In compositions with  $B = 500 \text{ kg/m}^3$ ,  $G_{Fm}$  has increased significantly up to 56 days. In compositions with  $B = 600 \text{ kg/m}^3$ , the  $G_{Fm}$  increase rate has markedly decreased in specimens with ages greater than 28 days. This indicates that the curing period of time needed to reach the maximum  $G_{Fm}$  decreases with the increase of the binder content.

c) In general,  $G_{Fm}$  decreases with the increase of the content of FA. However, for compositions with FA up to 40% and specimens with ages longer than 56 days this decrease is less noticeable.

d)  $G_{Fm}$  is substantially lower for mixtures with 60% FA; however, this tendency diminishes with the increase of the curing period of time.

e) Increasing the binder content from 500 kg/m<sup>3</sup> to 600 kg/m<sup>3</sup>, the  $G_{Fm}$  has decreased.

f)  $G_{Fm}$  increases with the age but the increase rate has decreased with time, in a similar trend like in compressive strength evolution.

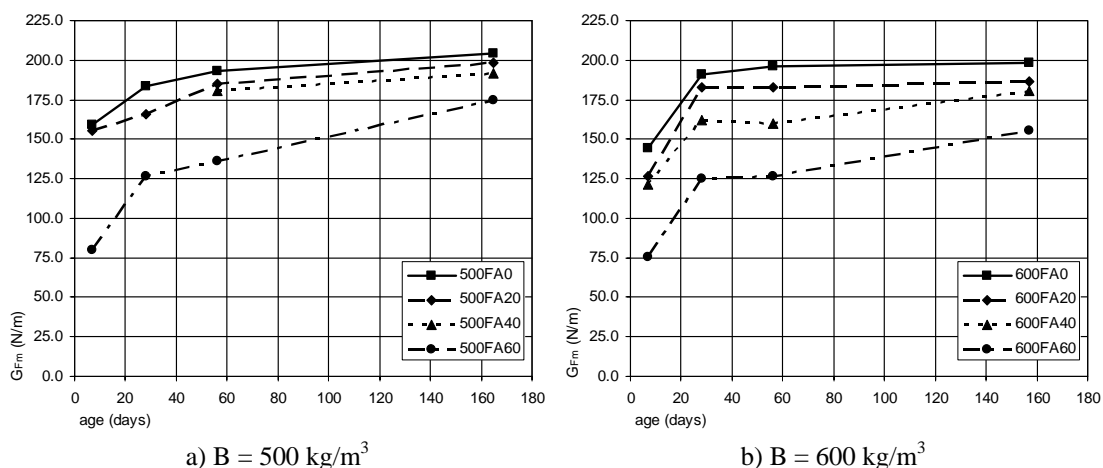


Fig. 5 – Influences of the age and percentage of cement replaced by fly ash on the fracture energy

Based on experimental evidence, the major part of the researchers has included the concrete compressive strength in their empirical approaches for the evaluation of the concrete fracture energy. In this line, CEB-FIP has recommended the following equation [14], [15]:

$$G_{Fm} = G_{F0} \left( \frac{f_{cm}}{f_{cm0}} \right)^{0.7} \quad (6)$$

The value of  $G_{F0}$  is determined from the maximum aggregate size (see table 4), and  $f_{cm0}$  is a constant equal to 10 MPa.

Table 4 –  $G_{F0}$  values

$D_{max}$ (mm)	$G_{F0}$ (N/mm)
8	0.025
16	0.03
32	0.058

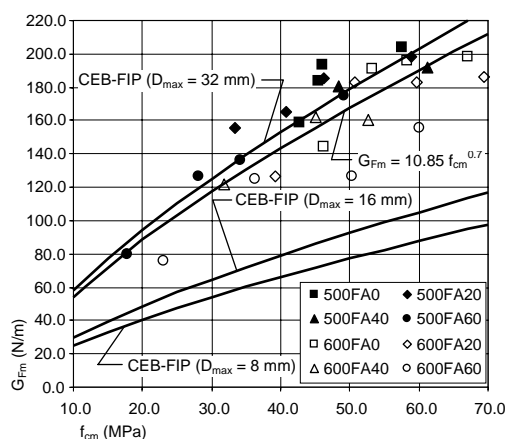


Fig. 6 – Relation between compressive strength and fracture energy

Figure 6 compares the experimental results with the curves predicted by equation (6) for maximum aggregate size of 8 mm, 16 mm and

32 mm. It is noted that CEB-FIP expression predicts values that are substantially smaller than the values obtained experimentally. The predicted values are similar to the experimental results only if  $D_{max}$  of 32 mm was considered. The aggregates of the present work, however, have a  $D_{max} = 9.53$  mm. For this  $D_{max}$  and interpolating  $G_{F0}$  from the values in table 4, it is obtained the following equation:

$$G_{Fm} = 5.18 f_{cm}^{0.7} \quad (7)$$

However, using equation (7) the  $G_{Fm}$  values are of about half the obtained experimental results. From regression analysis the following expression was obtained ( $R^2 = 63.68\%$ ):

$$G_{Fm} = 10.85 f_{cm}^{0.7} \quad (8)$$

The definition of the Equation (6) was only based on the area under the force-deflection curve. Other important aspects like the specimen dead weight were not taken into account. In the absence of experimental results, CEB-FIP [15] proposes equation (6) to evaluate  $G_{Fm}$ . This expression should only be used for concretes with a compressive strength lower than 80 MPa. According to CEB-FIP [14], equation (6) can cause deviations of  $G_{Fm}$  up to  $\pm 30\%$ .

#### 4.3. Modulus of elasticity in flexure

The influences of the percentage of FA and age on the modulus of elasticity in flexure,  $E_{cm,fl}$ , were represented in figure 7. From the analysis of this figure the following remarks can be pointed out:

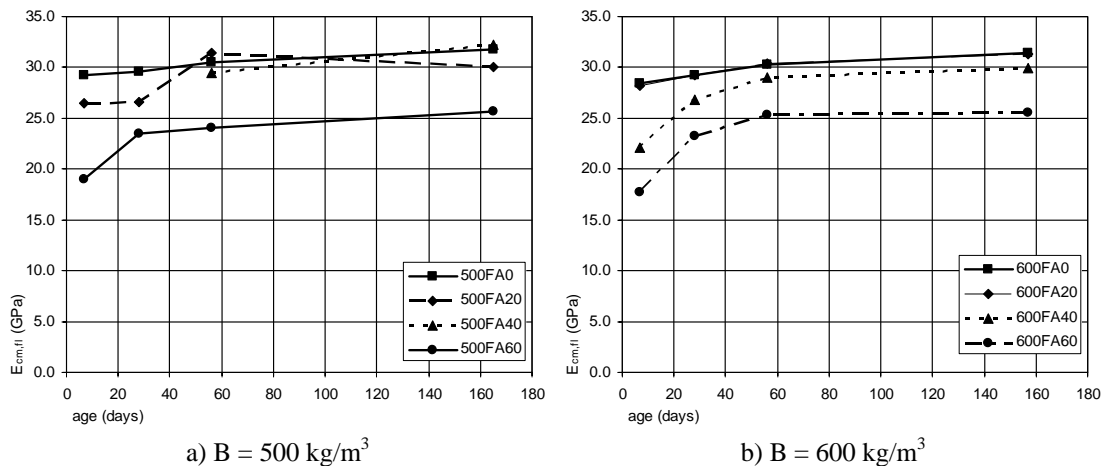


**Fig. 7** – Influences of the age and percentage of cement replaced by fly ash on the modulus of elasticity in flexure

a) The  $E_{cm,fl}$  of compositions without FA has an increase rate with the age significantly smaller than the increase rate registered in the compositions with FA.

b)  $E_{cm,fl}$  has decreased with the increase of the content of FA, mainly at lower ages.

c) For ages higher than 28 days, concretes with FA contents up to 40% present similar values of  $E_{cm,fl}$ .

d)  $E_{cm,fl}$  values of compositions with FA = 60% are significantly lower than  $E_{cm,fl}$  values of the remaining compositions.

the compressive strength is considered as the main influencing property.

The points in figure 8 represent the experimental relationship between the average compressive strength, determined in concrete cylinders,  $f_{cm}$ , and the corresponding flexural elasticity modulus,  $E_{cm,fl}$ , obtained in the bending tests. Curves of expressions proposed by ACI 363 committee [16], CEB-FIP [15] and Portuguese code (REBAP) [17] are also included in figure 8. These curves represent the relationship between the  $f_{cm}$  and the compressive elasticity modulus,  $E_{cm}$ .

The approach proposed by ACI is restricted to concretes of compressive strength between 21 MPa and 83 MPa, while in the equation of CEB-FIP no restrictions was made in terms of concrete strength class. REBAP is applicable for concretes up to 50 MPa of characteristic compressive strength, which correspond to a  $f_{cm}$  of about 58 MPa.

The results show that the values of  $E_{cm,fl}$  are, in general, lower than the corresponding estimated values of  $E_{cm}$  obtained by the application of the codes. So, for the designed compositions, the applicability of the referred expressions seems to overestimate the  $E_{cm,fl}$  values. ACI 363 equation is the one that comes closest to the obtained  $E_{cm,fl}$  experimental results.

CEB-FIP [15] suggests the adoption of a coefficient that takes into account the influence of the type of aggregate,  $\alpha_E$ . For quartzite aggregates used in the present work, CEB-FIP proposes a unit value for  $\alpha_E$ .

The  $\alpha_E$  value that gives the highest  $R^2$  (68.84%) in the regression analysis of the

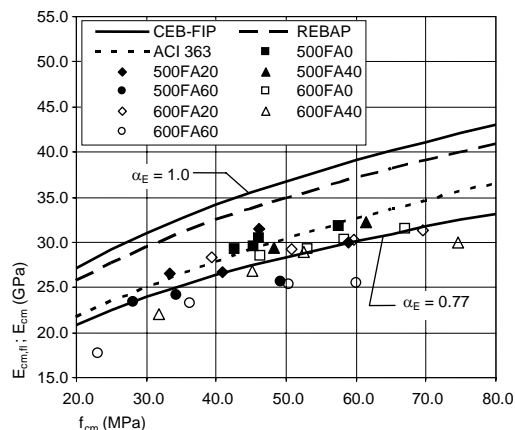


**Fig. 8** – Relation between experimental compressive strength, experimental elasticity modulus in flexure and estimated compressive elasticity modulus

The concrete elasticity modulus is controlled by the elasticity modulus of its components: hydrated binder paste and aggregates. The concrete elasticity modulus can be estimated from empirical expressions, where, in general,

obtained experimental results is 0.77. This value of  $\alpha_E$  is similar to the one proposed by CEB-FIP to estimate concrete's  $E_{cm}$  made with sandstone aggregates ( $\alpha_E = 0.7$ ).

## 5. CONCLUSIONS

The results showed that the addition of fly ash (FA) has decreased the values of the concrete mechanical properties, mainly when evaluated at young ages. This undesirable effect of FA decreases with the age of the concrete.

In general terms, at the age of about 56 days, the compressive strength and the flexural tensile behaviour of the compositions with FA content up to 40% (percentage of the binder weight) are not significantly different. This indicates that, from the economical and mechanical point of views, enhanced performance concrete can be designed with the use of relative high percentage of FA (less than 40% of the binder content) since live loads in a concrete structure are, in general, applied when the concrete is several months old.

In concrete compositions with 60% of binder replaced by FA, the values of the mechanical properties evaluated were considerably lower than the values of the corresponding reference series (0% of FA).

However, it is interesting to note the relatively high values of the mechanical properties at long curing times, achieved with such a high FA content.

In most cases, a good linear correlation was obtained between the evaluated mechanical properties (flexural tensile strength, fracture energy and modulus of elasticity in flexure) and the square root of compressive strength. This indicates that to an increase of the compressive strength corresponds a less pronounced increase of the tensile strength.

The equation proposed by CEB-FIP to estimate the concrete fracture energy is very conservative and the predicted values are about 50% of the obtained experimental values.

The concrete flexural modulus of elasticity can be satisfactory predicted using CEB-FIP expression if a correction factor, less than the unit value is introduced, in order to take into account distinct micro-failure modes (at micro/meso level point of view) mobilised at compression and flexural behaviour.

## 6. REFERENCES

- [1] Hordijk, D.A., "Local approach to fatigue of concrete", Dissertation (1991), Delft University of Technology, Holland.
- [2] RILEM, Draft Recommendation, 50-FMC Committee Fracture Mechanics of Concrete, "Determination of the fracture energy of mortar and concrete by means of three-point bending tests on notched beams", Materials and Structures, V. 85, N. 85, pp. 285-290 (1985).
- [3] Wang, Y., Li, V.C. and Backer, S., "Experimental determination of tensile behaviour of fibre reinforced concrete", ACI Materials Journal, V. 87, N. 5, pp. 461-468, September-October (1990).
- [4] EN450, "Fly Ash for concrete - definitions, requirements and quality control", CEN, September (1994).
- [5] ASTM C618, "Standard specification for coal fly ash and raw or calcined natural pozzolan for use as a mineral admixture in concrete", 1999 Annual Book of ASTM Standards, V. 04.02 - Concrete and Aggregates, July (1998).
- [6] Camões, A., Rocha, P., Pereira, J.C., Aguiar, B. and Jalali, S., "Low cost high performance concrete using low quality fly ash", 12<sup>th</sup> ERMCO Congress, Lisbon, pp. 478-486, June (1998).
- [7] Rocha, P., "High performance concrete using common materials and procedures", Master Thesis, University of Minho, October (1999) (*in Portuguese*).
- [8] Camões, A., "High performance concrete incorporating fly ash", Doctoral Thesis, University of Minho, July (2002) (*in Portuguese*).
- [9] Freitas, F., Barros, J., Fonseca, P., "Manual book of the structures testing system - SENTUR", University of Minho, 40 pp., September (1998) (*in Portuguese*).
- [10] Barros, J., Sena Cruz, J. "Fracture energy of steel fibre reinforced concrete", Journal of Mechanics of Composite Materials and Structures, V. 8, N. 1, pp. 29-45 (2001).
- [11] Barros, J., "Fibre reinforced concrete behaviour - experimental analysis and



numerical simulation”, Doctoral Thesis, FEUP, December (1995) (*in Portuguese*).

[12] Peterson, P.-E., “Crack growth and development of fracture zones in plain concrete and similar materials”, Lund Institute of Technology, Division of building materials, Report TVBM-1006.

[13] Hillerborg, A., “Concrete fracture energy tests performed by 9 laboratories according to a draft RILEM recommendation”, Report to RILEM TC50-FMC, Report TVBM-3015, Lund, Sweden (1983).

[14] CEB-FIP, “Model code 90 – design code”, Thomas Telford, pp. 437 (1990).

[15] CEB-FIP, “Structural concrete. Textbook on behaviour, design and performance, updated knowledge of the CEB/FIP model code 1990”, Volume 1, July (1999).

[16] ACI 363, “State-of-the-art report on high strength concrete”, Reported by Committee 363, American Concrete Institute (1992).

[17] REBAP, “Portuguese design code of reinforced and prestressed concrete structures”, Imprensa Nacional da Casa da Moeda, E.P., Lisbon (1986) (*in Portuguese*).